

For Excel and Matlab see end of document or Github:

<https://github.com/skabaria9/chemE5440-TakeHomeFinal>

Problem 1

See Excel Document "Problem1.xlsx" at end of document and on Github for full work for this problem.

1. Part A

Phosphofructokinase (PFK) catalyzes the conversion of D-fructose 6 - phosphate (F6P). PFK is strongly activated in the presence of 3'-5'-AMP.

Model (adapted from the generalized model described in the final): The overall rate of the PFK reaction can be modeled with $\hat{r}_1 = r_1 v_1(\dots)$ where \hat{r}_1 denotes the overall rate of the PFK reaction ($\mu M/h$).

r_1 denotes the kinetic limit in the absence of allosteric regulation,

$$r_1 = k_{cat} E_1 \left(\frac{F6P}{K_{F6P} + F6P} \right) \left(\frac{ATP}{K_{ATM} + ATP} \right) \quad (1)$$

where with substitution

| Parameter | Value | Units |
|-----------|-------|----------|
| k_{cat} | 1440 | h^{-1} |
| E_1 | 0.12 | μM |
| F6P | 0.1 | mM |
| K_{F6P} | 0.11 | mM |
| ATP | 2.3 | mM |
| K_{ATP} | 0.42 | mM |

$$r_1 = 69.6 \mu M/h \quad (2)$$

$v_1(\dots)$ denotes the allosteric regulation function ($0 \leq v_1 \leq 1$)

$$v_1(\dots) = \frac{W_1 + f_2 W_2}{1 + W_1 + f_2 W_2} \quad (3)$$

where W_i denotes the weight configuration (1 is for PFK, and 2 is for 3'-5'-AMP), and f_2 is the hill binding function for 3'-5'-AMP which describes the fraction of bound activator/inhibitor (x is 3'-5'-AMP concentration)

$$f_2 = \frac{\left(\frac{x}{K_2}\right)^{n_2}}{1 + \left(\frac{x}{K_2}\right)^{n_2}} \quad (4)$$

where K_2 is the binding constant for 3'-5'-AMP (mM) and n_2 is the order parameter for 3'-5'-AMP (dimensionless).

Find W_1

To estimate W_1 , we look at where concentration of 3'-5'-AMP = 0, $x = 0$; hence $f_2 = 0$, and we can simplify \hat{r}_1 and v_1 to

$$v_1(\dots) = \frac{W_1 + f_2 W_2}{1 + W_1 + f_2 W_2} \sim \frac{W_1}{1 + W_1} \quad (5)$$

$$\hat{r}_1 = r_1 v_1(\dots) = r_1 \frac{W_1}{1 + W_1} = 3.003 \mu M/h \quad (6)$$

Solving, $W_1 = 0.0451$ (dimensionless / unitless).

Find W_2

To estimate W_2 , we look at where concentration of 3'-5'-AMP is large, $x \rightarrow 1$, (specifically $x = 0.99 \mu M/h$). With the assumption that $(\frac{x}{K_2})^{n_2} \gg 1$, hence $f_2 \rightarrow 1$

$$f_2 = \frac{(\frac{x}{K_2})^{n_2}}{1 + (\frac{x}{K_2})^{n_2}} \sim \frac{(\frac{x}{K_2})^{n_2}}{(\frac{x}{K_2})^{n_2}} \sim 1 \quad (7)$$

and we simplify \hat{r}_1 and v_1 to:

$$v_1(\dots) = \frac{W_1 + f_2 W_2}{1 + W_1 + f_2 W_2} \sim \frac{W_1 + W_2}{1 + W_1 + W_2} \quad (8)$$

$$\hat{r}_1 = r_1 v_1(\dots) = r_1 \frac{W_1 + W_2}{1 + W_1 + W_2} = 68.653 \mu M/h \quad (9)$$

Substituting W_1 from before and solving, $W_2 = 74.03$ (dimensionless / unitless).

Note, if we do not make the assumption that $f_2 \rightarrow 1$ and vary both f_2 and W_2 for the best fit when $x = 0.99$, we solve that $f_2 = 0.9999$ and $W_2 = 74.03$. This confirms that the assumption $f_2 = 1$ with large concentration of 3'-5'-AMP (x) is correct.

2. Part B

Using the full form of the equations for \hat{r}_1 , f_2 , and $v_1(\dots)$ as defined in PART A (Equations (1), (3), and (4)), I performed a least squares fit to estimate the values of K_2 and n . The excel files shows the in depth work. In brief, I iterated through values of K_2 and n using Excels Solver tool, until the sum of the squared differences between the calculated theoretical value of \hat{r}_1 and the measured rate for all concentrations x was minimized:

$$\min(\sum (\hat{r}_{1,measured} - \hat{r}_{1,calculated})^2) \quad (10)$$

The summarized least square fit parameters are:

| Parameter | Value | Units |
|-----------|-------|---------------|
| W_1 | 0.045 | dimensionless |
| W_2 | 74.03 | dimensionless |
| K_2 | 0.657 | mM |
| n | 2.49 | dimensionless |

3. Part C

The Overall Calculated Rate ($\mu M/h$) was plotted over the Overall Measured Rate ($\mu M/h$), the latter of which was plotted with its 95% confidence interval (see below). As seen from the graph below, for most data points, the calculated rate falls within the 95% interval of the measured rate data. For a few points, the calculated and measured points almost overlap, indicating that the model provided a good prediction of the allosteric regulation of PFK by 3'-5'-AMP in real cells.

The proposed model formulation *can* describe the data.

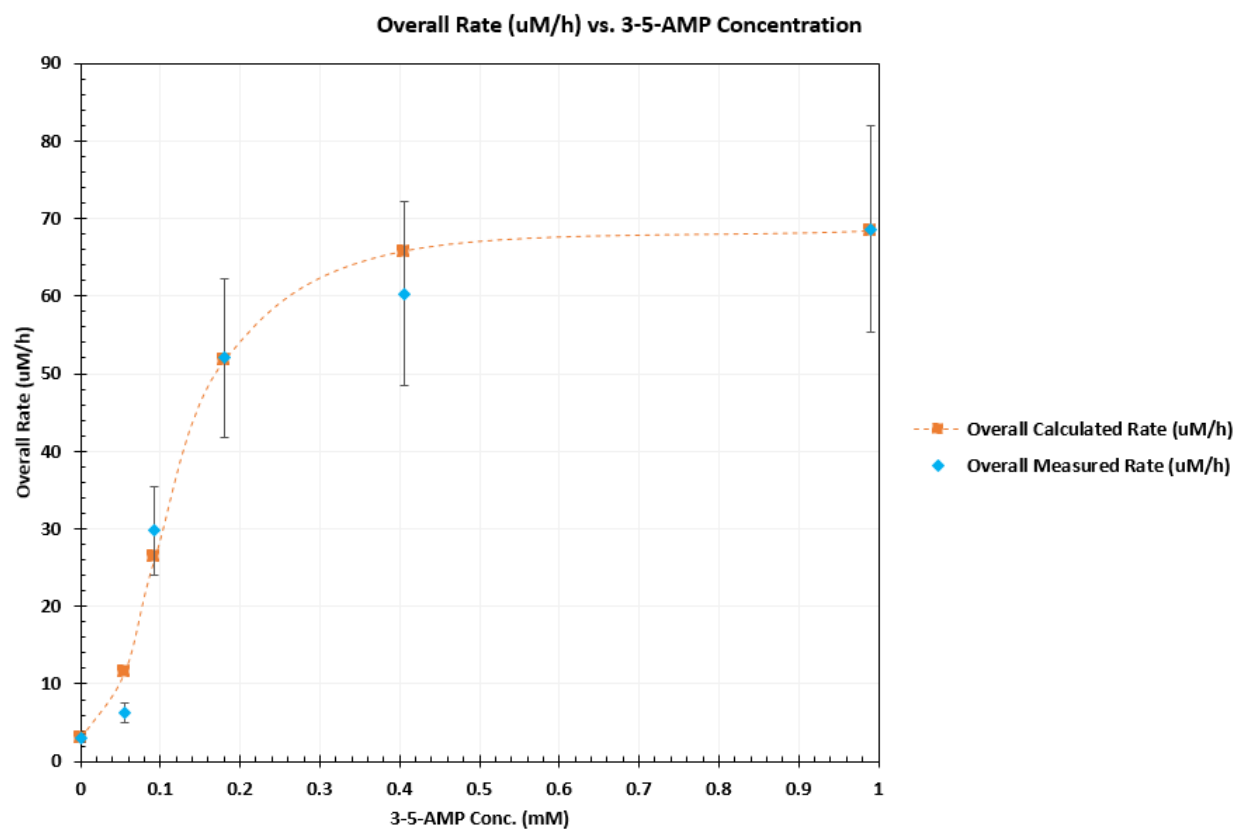


Figure 1: 1c. Plot of Overall Rate vs. 3'-5'- AMP Concentration. Error bars represent 95% Confidence Interval of Measured Data

Problem 2

See Matlab code at the end of this document and on Github for Problem 2.

1. Part A

We have the following toggle switch and conditions of bistability understood with the following dimensionless model for the network:

$$\frac{du}{dt} = \frac{\alpha}{1 + v^n} - u = f(u, v) \quad (11)$$

$$\frac{dv}{dt} = \frac{\alpha}{1 + u^n} - v = g(u, v) \quad (12)$$

where

- (a) u is the concentration of repressor for gene expression of v , and v is the concentration of repressor for gene expression for u
- (b) The term α is the "effective rate of synthesis of repressor" for u and v respectively. This is the lumped parameter that describes the net effect of RNA polymerase binding, open-complex formation, transcript elongation, transcript termination, repressor binding, ribosome binding and polypeptide elongation.
- (c) n is the cooperativity of repression
- (d) 1 is the degradation rate constant for repressor – hidden in the model equations above. The degradation term is $-\gamma_{deg,u}u$ and $-\gamma_{deg,v}v$ for u and v respectively. Above, the degradation terms are $-u$ and $-v$ for u and v respectively, implying that $\gamma_{deg,u} = \gamma_{deg,v} = 1$.

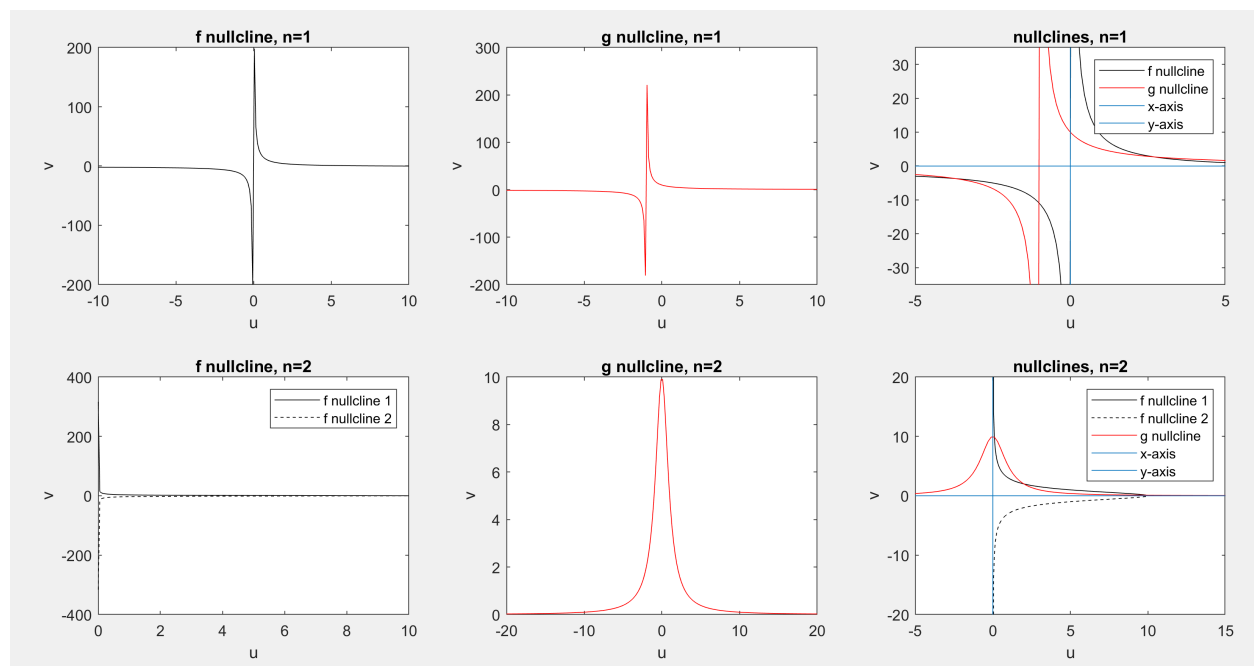


Figure 2: Nullclinesa when $n=1$ and $n=2$.

2. Part B

Plot of the nullclines where $f(u, v) = g(u, v) = 0$. See attached MatLab codes for analysis.

$n = 1$: As seen from the graphs and when solved on Matlab, when the $f(u, v)$ and $g(u, v)$ nullclines intersect when $u = -3.7$ and $u = 2.7$. (As you might see in the graph, there is another intersection when $u < 0$, however it is when the graph is asymptotic (probably undefined), so that is why it is excluded in this analysis. There are two total steady-state solutions, but because concentrations are always positive ($u > 0$ and $v > 0$), this means there is one physically feasible steady-state solution when $n = 1$.

$n = 2$: As seen from the graphs and when solved on Matlab, when the $f(u, v)$ and $g(u, v)$ nullclines intersect when $n = 2$, $u = 9.9$, $u = 0.10$, $u = -1 - 2i$, and $u = -1 + 2i$. There are three steady-states here because when $n > 1$ the nullclines form a sigmoidal shape which is what causes them to intersect three times. Because concentrations are always positive ($u > 0$ and $v > 0$) and not complex, this means there are three steady-state solutions when $n = 2$.

We observe that increasing the degree of cooperativity from $n=1$ to $n=2$ increases the number of solutions.

3. Part C

Steady-states were identified (they are circled) on stream plots constructed on Wol-

fram Alpha (example code and resulting graphs is screenshotted and included below). Steady-states were identified as areas with apparent "sinks," "sources," or "saddles." The steady-states are roughly circled on the stream plots. On MatLab the Steady-States u_S and v_S were numerically calculated by solving the system of equations $f(u, v) = 0, g(u, v) = 0$ at the conditions where $n = 1$ and $n = 2$. The numerical steady-states matched the behavior seen on the stream plots. Below, after the stream plots, tables summarize the results for each value of n .

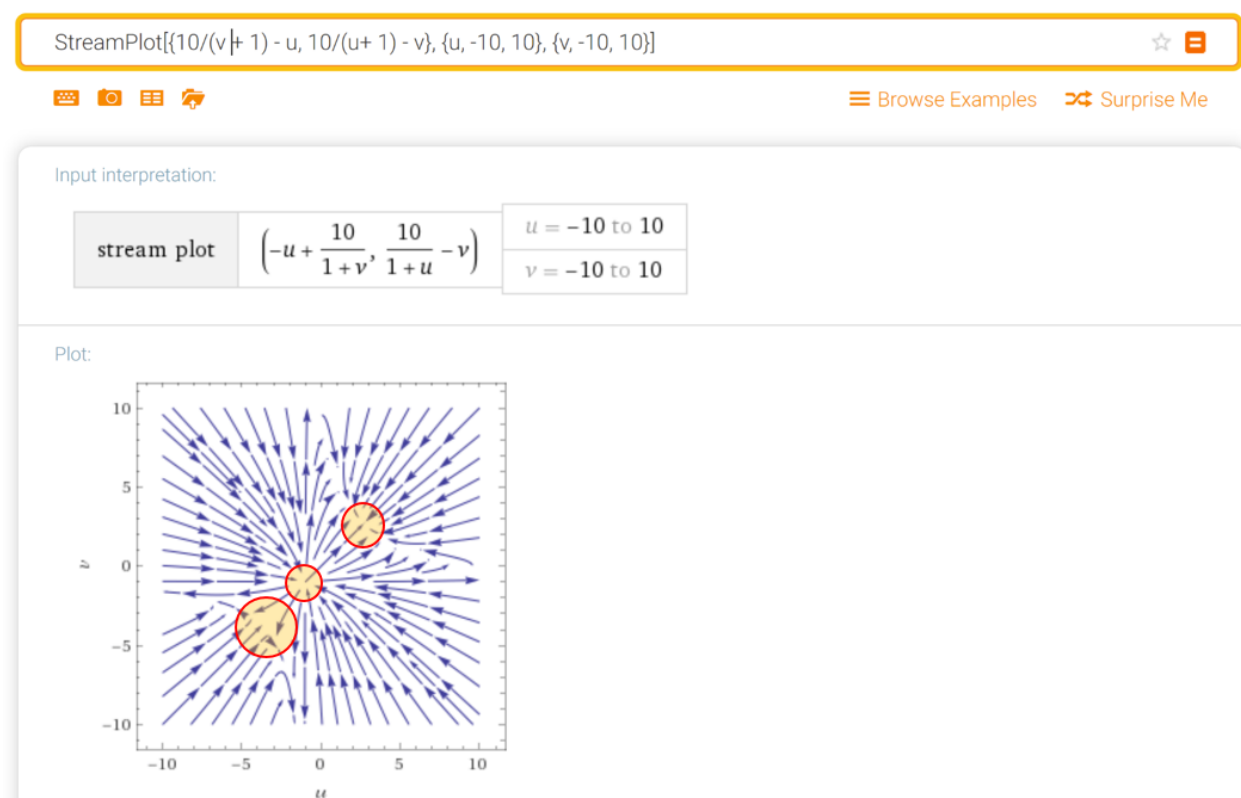


Figure 3: StreamLines when n=1.

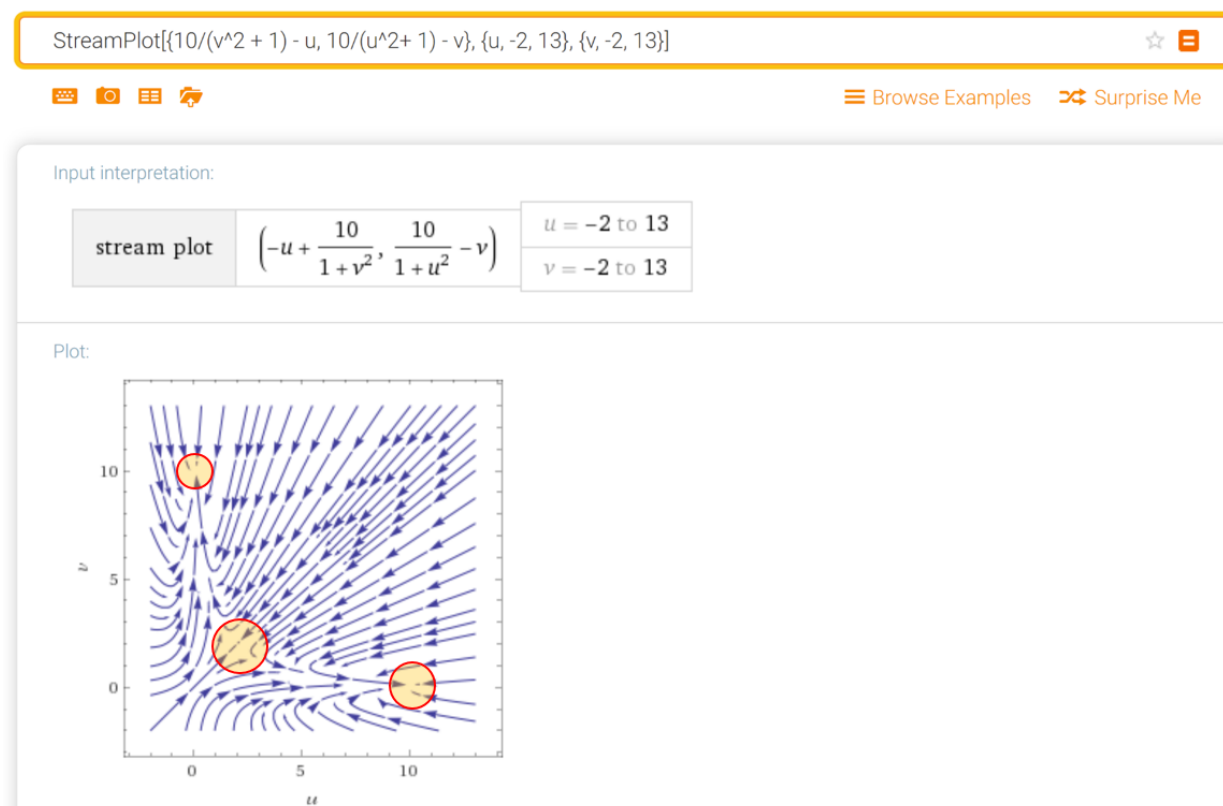


Figure 4: Streamlines when $n=2$.

The previous pages show the stream plots of $f(u, v)$ and $g(u, v)$. The stream plots shows vectors with size coordinates $(f(u, v), g(u, v))$ which represent the direction/speed that the concentrations of u and v will change over time depending on their starting concentration $u_{initial}$ and $v_{initial}$ which are the start point for the vector on the stream plots.

The following tables show the steady-states and their stability as inferred from the stream plots.

The steady states are as follows for $n=1$

| | u_S | v_S | stability |
|-------------------------------|-------|-------|-----------------|
| SS1 | 2.7 | 2.7 | stable |
| SS2 (not physically feasible) | -3.7 | -3.7 | unstable,saddle |

Note: there also appears to be a third unstable steady state around $u = -1$ and $v = -1$; this steady-state and SS2 above are not physically relevant because inhibitor concentrations must be ≥ 0 .

For $n = 1$ there is only one stable steady-state.

The steady states are as follows for $n=2$

| | u_S | v_S | stability |
|-----|------------------|------------------|------------------|
| SS1 | 2 | 2 | unstable, saddle |
| SS2 | 0.1010 | $9.8990 \sim 10$ | stable |
| SS3 | $9.8990 \sim 10$ | 0.1010 | stable |

As mentioned, there are three steady-states here because when $n = 2$ the nullclines form a sigmoidal shape and hence intersect three times. Here, we see that there are two stable steady-states and one unstable steady-states. The side of the unstable steady-state that u and v begin at determine the "basin" that they begin in and hence which stable steady which be approached. These "basins" can be observed qualitatively on the stream plots.

Summary of Influence of Co-operativity

Overall, from these results we can infer that the bi-stability of the system depends on the cooperativity n of the system. In other words, there must be $n > 1$ for two stable steady-states and one unstable steady-state. As described above, if $n = 1$ there is only one physically feasible stable steady state.

4. Part D

Consider a small perturbation around the steady-state. Define the differences from the steady-state as: $a = u - u_S$ and $b = v - v_S$, where u_S and v_S are the steady-state concentrations of u and v respectively.

The Taylor-Series expansion in one-dimension for $dA/dt = f(A)$ with $z = A - A_S$,

$$f(A) = f(A_S) + \frac{\delta f}{\delta A}|_{A_S}(A - A_S) + O((A - A_S)^2) \sim \frac{\delta f}{\delta A}|_{A_S}z \quad (13)$$

So, by analogy in two-dimensions:

$$\frac{da}{dt} = \frac{\delta f(u, v)}{\delta u}|_{(u_S, v_S)}a + \frac{\delta f(u, v)}{\delta v}|_{(u_S, v_S)}b = f_u a + f_v b \quad (14)$$

$$\frac{db}{dt} = \frac{\delta g(u, v)}{\delta u}|_{(u_S, v_S)}a + \frac{\delta g(u, v)}{\delta v}|_{(u_S, v_S)}b = g_u a + g_v b \quad (15)$$

To construct the Jacobian, then find the partial derivatives of f and g .

$$f_u = -1; f_v = \frac{\alpha n v^{n-1}}{(v^n + 1)^2} \quad (16)$$

$$g_u = \alpha n u^{n-1}(u^n + 1)^{-2}; g_v = -1 \quad (17)$$

Then the Jacobian is

$$\mathbf{J} = \begin{pmatrix} f_u & f_v \\ g_u & g_v \end{pmatrix} = \begin{pmatrix} -1 & \frac{\alpha n v^{n-1}}{(v^n + 1)^2} \\ \frac{\alpha n u^{n-1}}{(u^n + 1)^2} & -1 \end{pmatrix} \quad (18)$$

where

$$\mathbf{x} = \begin{pmatrix} a \\ b \end{pmatrix} \quad (19)$$

$$\mathbf{J}\mathbf{x} = \dot{\mathbf{x}} = \begin{pmatrix} da/dt \\ db/dt \end{pmatrix} = \begin{pmatrix} d(u_S + a)/dt \\ d(v_S + b)/dt \end{pmatrix} = \begin{pmatrix} du/dt \\ dv/dt \end{pmatrix} \quad (20)$$

Stability Analysis

To analyze stability, then find the trace and determinant:

$$tr(\mathbf{J}) = f_u + g_v = -1 + -1 = -2 \quad (21)$$

$$det(\mathbf{J}) = f_u g_v - f_v g_u = (-1)(-1) - \left(\frac{\alpha n v^{n-1}}{(v^n + 1)^2}\right)\left(\frac{\alpha n u^{n-1}}{(u^n + 1)^2}\right) \quad (22)$$

$$det(\mathbf{J}) = 1 - \left(\frac{\alpha n v^{n-1}}{(v^n + 1)^2}\right)\left(\frac{\alpha n u^{n-1}}{(u^n + 1)^2}\right) \quad (23)$$

Next, substitute for the center steady-state where $u = u_S$, $v = v_S$, and $u_S = v_S$ for the determinant,

$$det(\mathbf{J}) = 1 - (\alpha n u_S^{n-1}(u_S^n + 1)^{-2})^2 \quad (24)$$

Further simplify

$$\det(\mathbf{J}) = 1 - \frac{\alpha^2 n^2 u_S^{2n-2}}{(u_S^n + 1)^4} \quad (25)$$

From the Poincare diagram, in the region $\text{tr}(\mathbf{J}) < 0$ (which we are in since $\text{tr}(\mathbf{J}) = -2$ for all n, α, u_S), we must have $\det(\mathbf{J}) \geq 0$ for stability.

Therefore, for stability:

$$\frac{\alpha^2 n^2 u_S^{2n-2}}{(u_S^n + 1)^4} \leq 1 \quad (26)$$

and for **un**stability

$$\frac{\alpha^2 n^2 u_S^{2n-2}}{(u_S^n + 1)^4} > 1 \quad (27)$$

Influence of Degree of Cooperativity on Stability of Center Steady-State

The change of the cooperativity from $n < 1$ to $n > 1$ will affect whether there is an additional u_S term in the denominator and no u_S term in the numerator (which happens when $n < 1$ and hence exponent $2n - 1 < 0$), only in the term $(u_S + 1)^{-4}$ (which happens when $n = 1$ and hence exponent $2n - 1 = 0$), or an u_S term in the numerator in addition to the $(u_S + 1)^4$ term in the denominator (which happens when $n > 1$ and hence exponent $2n - 1 > 0$).

If u_S only appears in the denominator it makes the value of the fraction smaller, and there are more values of α and u_S that would satisfy $\frac{\alpha^2 n^2 u_S^{2n-2}}{(u_S^n + 1)^4} \leq 1$. Similarly, if there is a u_S in the numerator it makes the value of the fraction larger, and there are more values of α and u_S that would satisfy $\frac{\alpha^2 n^2 u_S^{2n-2}}{(u_S^n + 1)^4} > 1$.

Therefore, a smaller n (or more specifically $n \leq 1$) probably leads to a stable center steady-state, but a larger steady state (or more specifically $n > 1$) probably leads to an unstable center steady-state.

Influence of Rate of Synthesis on Stability of Center Steady-State

The stability criteria can be rearranged to analyze the effect of rate of synthesis α . For stability:

$$\alpha^2 \leq \frac{(u_S^n + 1)^4}{n^2 u_S^{2n-2}} \quad (28)$$

and for **un**stability

$$\alpha^2 > \frac{(u_S^n + 1)^4}{n^2 u_S^{2n-2}} \quad (29)$$

From these criteria, it is easy to infer that for small α there are more values of n and u_S that would lead to a stable center steady-state. For large α there are more values of n and u_S that would lead to a *un*stable center steady-state.

5. **Part E**

Use MatLab to calculate the numerical eigenvalues for $\alpha = 10$, $n = 1$, and $n = 2$ with the following formula for eigenvalues from class:

$$\lambda_{1,2} = \frac{tr(\mathbf{J}) \pm \sqrt{tr(\mathbf{J})^2 - 4det(\mathbf{J})}}{2} \quad (30)$$

and the values of $tr(\mathbf{J})$ and $det(\mathbf{J})$ from the PART D. Please see the Matlab code for the full work.

For $n = 1$, the center steady state is "SS1" in Part C, $u_S = 2.7, v_S = 2.7$.

For $n = 2$, the center steady state is "SS1" in Part C. $u_S = 2, v_S = 2$

The summarized results of the eigenvalues in both cases, as solved in Matlab:

| n | $u_S = v_S$ | $tr(\mathbf{J})$ | $det(\mathbf{J})$ | λ_1 | λ_2 |
|---------|-------------|------------------|-------------------|-------------|-------------|
| $n = 1$ | 2.7 | -2 | 0.4664 | -0.2610 | -1.7305 |
| $n = 2$ | 2 | -2 | -1.56 | 0.60 | -2.60 |

There are two negative eigenvalues when $n = 1$ indicating stability. There is one positive and one negative eigenvalue for $n = 2$ indicating instability with saddle behavior (based on the tr and det and the Poincare diagram).

The change in cooperativity from $n = 1$ to $n = 2$ led to the change of one of the eigenvalues from "all negative" to "one positive and one negative", and hence the changing of the center steady state from stable to unstable.

Increasing the cooperativity led to a change from a stable center steady-state to an unstable center steady-state.

6. **Part F-1** Fast equilibrium implies for equations (3)-(5) in the final document the $\frac{d}{dt} = 0$. By hand, this assumption was applied to solve for $\frac{dR_i}{dt}$. The work is shown on the next page.

2f-1

$$\frac{dR_i^*}{dt} = k_s L R_i - k_r R_i^* = 0 \rightarrow k_s L R_i = k_r R_i^* \quad (1)$$

$$R_i^* = \frac{k_s L}{k_r} R_i$$

$$\frac{dN_i^*}{dt} = k_s^{ND} N_i D_j - k_r^{ND} N_i^* = 0 \Rightarrow k_s^{ND} N_i D_j = k_r^{ND} N_i^* \quad (2)$$

$$\frac{dD_j}{dt} = k_d R_j^* - \gamma_0 D_j = 0 \rightarrow k_d R_j^* = \gamma_0 D_j$$

$$\frac{k_d R_j^*}{\gamma_0} = D_j \quad (3)$$

$$\text{from (1)} \rightarrow R_j^* = \frac{k_s L}{k_r} R_j \quad (4)$$

$$(3) \text{ and } (4) \rightarrow D_j = \frac{k_d k_s L}{k_r \gamma_0} R_j \quad (5)$$

Figure 5: 2f part1

from the question part

$$\frac{dR_i}{dt} = \frac{\beta^n}{K^n + N_i^{*n}} - \gamma_R R_i$$

sub-in (2)

$$\frac{dR_i}{dt} = \frac{\beta^n}{K^n + \left(\frac{K_s^{ND} N_i D_j}{K_r^{ND}} \right)^n} - \gamma_R R_i$$

sub-in (5)

$$\frac{dR_i}{dt} = \frac{\beta^n}{K^n + \left(\frac{K_s^{ND} N_i k_D k_S L}{k_R \gamma_D} R_j \right)^n} - \gamma_R R_i \quad (6)$$

sub-in $(i,j) = (1,2)$ and $(2,1)$ to find equations for # 2f-1

$$\frac{dR_1}{dt} = \frac{\beta^n}{K^n + \left(\frac{K_s^{ND} N_1 k_D k_S L}{k_R \gamma_D} R_2 \right)^n} - \gamma_R R_1$$

$$\frac{dR_2}{dt} = \frac{\beta^n}{K^n + \left(\frac{K_s^{ND} N_2 k_D k_S L}{k_R \gamma_D} R_1 \right)^n} - \gamma_R R_2$$

Figure 6: 2f part1 (continued)

From the work by hand:

$$\frac{dR_1}{dt} = \frac{\beta^n}{K^n + \left(\frac{k_f^{ND} N_1 k_D k_f L}{k_r \gamma_D} R_2\right)^n} - \gamma_R R_1 \quad (31)$$

$$\frac{dR_2}{dt} = \frac{\beta^n}{K^n + \left(\frac{k_f^{ND} N_2 k_D k_f L}{k_r \gamma_D} R_1\right)^n} - \gamma_R R_2 \quad (32)$$

7. Part F-2

Non-dimensionalize with $u = R_1/K$, $v = R_2/K$, and $\tau = \gamma_R t$. Re-arranging, substitute in $R_1 = Ku$, $R_2 = Kv$, and $\gamma_R = \tau/t$ to $\frac{dR_1}{dt}$.

$$\frac{dKu}{dt} = \frac{\beta^n}{K^n + \left(\frac{k_f^{ND} N_1 k_D k_f L}{k_r \gamma_D} Kv\right)^n} - \frac{\tau}{t} Ku \quad (33)$$

By simplifying you get the following:

$$K \frac{du}{dt} = \frac{\beta^n}{K^n + K^n \left(\frac{k_f^{ND} N_1 k_D k_f L}{k_r \gamma_D} v\right)^n} - \frac{\tau}{t} Ku \quad (34)$$

$$K \frac{du}{dt} = \frac{\beta^n}{K^n \left(1 + \left(\frac{k_f^{ND} N_1 k_D k_f L}{k_r \gamma_D} v\right)^n\right)} - \frac{\tau}{t} Ku \quad (35)$$

$$K \frac{du}{dt} = \frac{\left(\frac{\beta}{K}\right)^n}{1 + \left(\frac{k_f^{ND} N_1 k_D k_f L}{k_r \gamma_D}\right)^n v^n} - \frac{\tau}{t} Ku \quad (36)$$

By analogy:

$$K \frac{dv}{dt} = \frac{\left(\frac{\beta}{K}\right)^n}{1 + \left(\frac{k_f^{ND} N_1 k_D k_f L}{k_r \gamma_D}\right)^n u^n} - \frac{\tau}{t} Kv \quad (37)$$

The last two simplifications of the non-dimensionalized form are analogous to equations presented at the beginning of Problem 2:

$$\frac{du}{dt} = \frac{\alpha}{1 + v^n} - u \quad (38)$$

and the analysis of stability at the uniform state $u = v$ from parts 2a-e can be applied here as well.

Since, the ligand VEGF (L) is in the denominator of the first term, it can by analogy be considered a part of the rate of synthesis α . Looking at a supposed lumped term of α/L where here $\alpha \sim \left(\frac{\beta}{K}\right)^n$, increasing L would therefore decrease α . As seen in Part E, a smaller α would lead to a stable uniform (a.k.a. center) steady state. Decreasing L

hence increases α . As seen in Part E, a larger α would lead to an unstable uniform (a.k.a. center) steady state.

Briefly, small $L \rightarrow$ unstable uniform steady-state; and large $L \rightarrow$ stable uniform steady-state. This makes sense, since you would want a more sensitive (unstable) system if there is not currently too much ligand VEGF and you want there to be a response "tip-cell" if a little VEGF-R were to enter a system. If there is a lot of ligand VEGF already in the system, you want the system to be patterned and each type of cell stably presenting its given characteristics (of either notch or delta.)

Other ways to Affect System:

To drive the system to instability you could also manipulate in the following ways:

- increase β which is analogous to synthesis rate α ; increase $\alpha \rightarrow$ instability (from Part E)
- by genetic engineering, decrease binding coefficient K which is also analogous to α because β/K is in the numerator of the non-dimensionalized equation; increase $\alpha \rightarrow$ instability (from Part E)
- by genetic engineering, make n small ($\sim n < 1$); from Part E, $n \leq 1 \rightarrow$ instability
- If it were possible to engineer some of the rates of the system: increasing $k_f^{ND}, N1, N2, k_D, k_I$ or decreasing k_r, γ_D would lead to instability